FORERUNNERS: OUTER RIMS OF SOLAR CORONAL TRANSIENTS

B. V. JACKSON* and E. HILDNER

*High Altitude Observatory, National Center for Atmospheric Research**, Boulder, Colo. 80307, U.S.A.*

(Received 3 April; in revised form 27 July, 1978)

Abstract. The large loop or blob-like transient events viewed in the white-light corona are rimmed by broad regions where the density is slightly enhanced above the pre-transient corona. Every one of the Skylab events studied for which sufficiently good Skylab coronagraph coverage is available shows this effect. The upper boundaries of these 'forerunners' blend gradually into the background corona 1 to $\geq 2R_{\odot}$ above the transients' leading edges. In any single event, the coronal mass enhancement represented by the forerunner comprises up to 25% of the total excess mass present in the coronagraph's field of view and includes a much larger volume of the corona than previously attributed to the underlying transient. We have not yet seen a forerunner without an accompanying transient. Clearly, forerunners must be reckoned with in any proposed models of discrete outward coronal mass motions, because they indicate the presence of disturbed corona far ahead of the denser portions of the event.

1. Introduction

The large scale loop or blob-like coronal transients observed in coronagraph images (e.g., Figure 1) are generally interpreted as material that eventually escapes from the solar vicinity (e.g., Gosling *et al.*, 1974; or for review see Holzer, 1977). Continuous ejections of ionized gas from the Sun were hypothesized as early as the work of Chapman and Ferraro (1931). Bartels (1937) suggested that geomagnetic storms which follow approximately 24 hr after solar eruptions are caused by the erupting material ejected from the Sun. However, only when concurrent observations were accumulated from space satellites and ground-based instruments could the nature and frequency of these ejections be determined (e.g., Hundhausen *et al.*, 1970; Tousey, 1973; Koomen *et al.*, 1974; Stewart *et al.*, 1974; Gosling *et al.*, 1974).

For the purposes of this paper, we define a transient to be a loop or blob-like structure seen moving outward from the Sun on consecutive coronagraph images. Distinct from this in our interpretation is the transient forerunner, a region rimming the transient where the density is slightly enhanced over the pre-event state. This rim of excess mass lies around what is generally described as the transient's leading edge. The arrow in Figure 1 depicts the leading edge of a typical transient (see also Gosling *et al.*, 1976).

Earlier papers indicated the presence of forerunners around particular events. Gosling *et al.* (1974) note that a streamer adjacent to the 10 August 1973 transient is

* Skylab Solar Workshop Postdoctoral Appointee 1975–78. The Skylab Solar Workshops are sponsored by NASA and NSF and managed by the High Altitude Observatory. Present address, CSIRO, Division of Radiophysics, Sydney, Australia.

** The National Center for Atmospheric Research is sponsored by the National Science Foundation.

Solar Physics **60** (1978) 155–170.

Fig. 1. A brighter than average loop-like eruption of material photographed at 14:48 UT 10 August 1973 by the HAO orbiting coronagraph aboard Skylab. The Sun is obscured by an occulting disk at image center whose effective radius is $1.6R_\odot$; the outer edge of the field of view is $6R_\odot$. The strong gradient of coronal radiance has been vignetted by the instrument. An arrow indicates the leading edge of the transient. Note the streamer to the south of the event bent in the shape of the underlying material (first described by Gosling *et al.*, 1974).

bent in a shape which conforms to the underlying dense material. Hildner *et al.* (1975a) remark that the 10 June 1973 event shows a streamer which is disturbed ahead of the transient and a faint feature $0.6R_\odot$ in front of the transient's leading edge. Dulk *et al.* (1976), in digital subtractions of a pre-transient photograph from later images containing the transient of 15 September 1973, more nearly indicate the true extent of the coronal disruption; they show what we call a forerunner and interpret it as part of a bow wave or the region behind a shock.

In this paper we report the results of digital analysis of 21 transient events observed with HAO's orbiting coronagraph on board Skylab. For 18 of these events

(about one quarter of the 77 transients identified on coronagraph images) the data show obvious broad rims of excess density bordering the transients – forerunners. The apparent one to one correspondence between a forerunner and its transient implies that a forerunner-transient pair comprises one event. Further, we show that at any one time a forerunner's excess density decreases with distance from its transient's leading edge; in some instances forerunners extend $\geq 2R_\odot$ above their underlying transients. In the remainder of the Observations section of the paper we discuss the precision of digital subtractions and we describe tests which confirm the validity of our results. The Discussion section contains arguments tending to discredit the explanation of forerunners as merely the coherent expansion of the lower corona. Two other possibilities, namely, that the forerunner is a local, *in situ* compression of material which is perhaps compressed, penetrated, and left behind by the material ejection, or that it is a piecemeal material ejection over a long period of time are contrasted. We leave for a later paper (Jackson, 1979) descriptions of the temporal relation between forerunner and surface material motion and observations pertaining to the origin of forerunners.

2. Observations

A Skylab coronagraph image which shows a loop-like transient of greater than average brightness is displayed in Figure 1. (For a description of the Skylab coronagraph, see MacQueen *et al.* (1974).) No point in this image has a recorded radiance greater than 1.4 times that point's pre-event recorded radiance. In other words, transients observed with the Skylab coronagraph are recorded as low-contrast phenomena. Sensitivity to the part of the corona that changes during a transient can be enhanced by differencing techniques. Comparison of images can be performed quantitatively by digitizing a pre-event image and subtracting it from subsequent digitized images to create resultant images. To first order, this technique eliminates the unaffected coronal and instrumental stray radiance. The resultant images show only the changes which accompany a transient event and form the basis for the analysis presented in this paper. To display the characteristics of transients and their forerunners, we convert the resultant images (which show brightness changes) to diagrams of excess columnar density. At any one height, excess columnar density is directly proportional to the brightness difference shown in the resultant image. The conversion technique, described more completely by Hildner *et al.* (1975a), assumes that the material contributing to these events' additional brightness is located in the plane of the sky.

Three typical transients and their forerunners are depicted in Figures 2a to 2d. To consistently distinguish a forerunner from the unaffected corona, we define the outer boundary of a forerunner as the 6×10^{-9} g cm^{-2} contour level of excess columnar density (the line between stippled and clear areas in Figure 2b–c). This value corresponds to $1 \times 10^{-10}\ B_\odot$ at a height of $2R_\odot$ and to $1 \times 10^{-11}\ B_\odot$ at $6R_\odot$, where $B_\odot$ and $R_\odot$ are the mean solar radiance and solar radius, and represents the 2σ level of

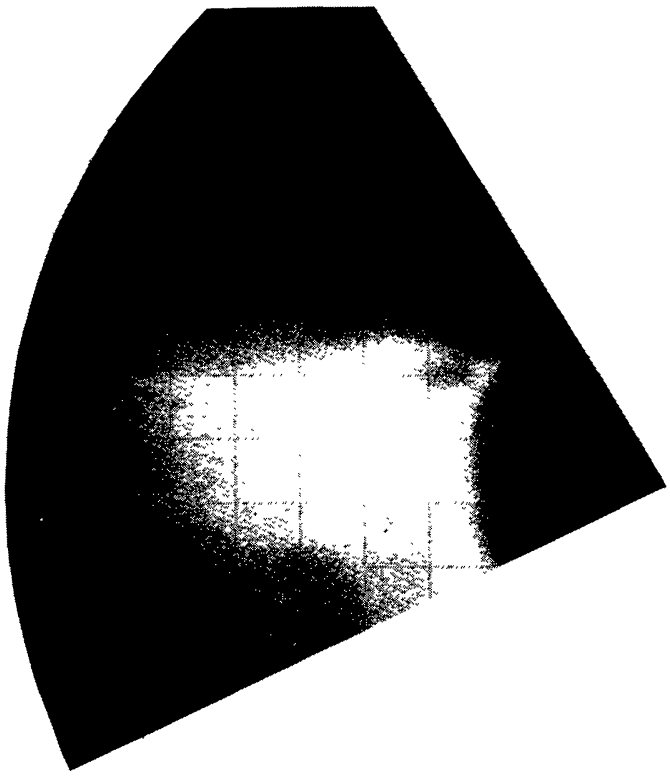

Fig. 2a. The event of 19 December 1973 photographed at 08:05 UT. Sun center is on the right, solar north is to the top, east to the left. The image has been cropped to match the digital subtraction of Figure 2b. The loop-like transient at $3.5R_{\odot}$ is progressing outward at an apparent speed of 100 km s^{-1}.

noise in resultant images. Of course, the region of disturbed corona actually extends beyond this arbitrary outer boundary to some unmeasureable boundary at the zero level contour. The majority of transients in this study are observed to have a sharp outer edge. That is, at the transient's leading edge, there is a steepening or break in the gradient of excess columnar density which separates the transient from the forerunner. For many events this transient-forerunner boundary occurs at approximately the 50×10^{-9} g cm^{-2} contour of excess columnar density. The inset at the border of Figure 2c depicts the excess columnar density along a scan through an event and gives an example of the abrupt change in density gradient at the transient's outer edge. In all events, we choose the 50×10^{-9} g cm^{-2} contour of excess mass as a working definition of the boundary between the transient's leading (outer) edge and the forerunner's trailing (inner) edge. In Figures 2b–d this edge is depicted by the boundary between the lightly and darkly stippled areas.

For contrast, we have assembled events in Figure 2 which have speeds ranging from 100 km s^{-1} to 850 km s^{-1}. The event of 10 January 1974 is especially interesting, because from polarization measurements it appears to be a loop seen edge on (Munro, 1978). The forerunner bordering this loop may be compared with those bordering the 19 December and 17 January events. That the forerunner in the 10 January event is not as extensive in position angle at any given height as the others in

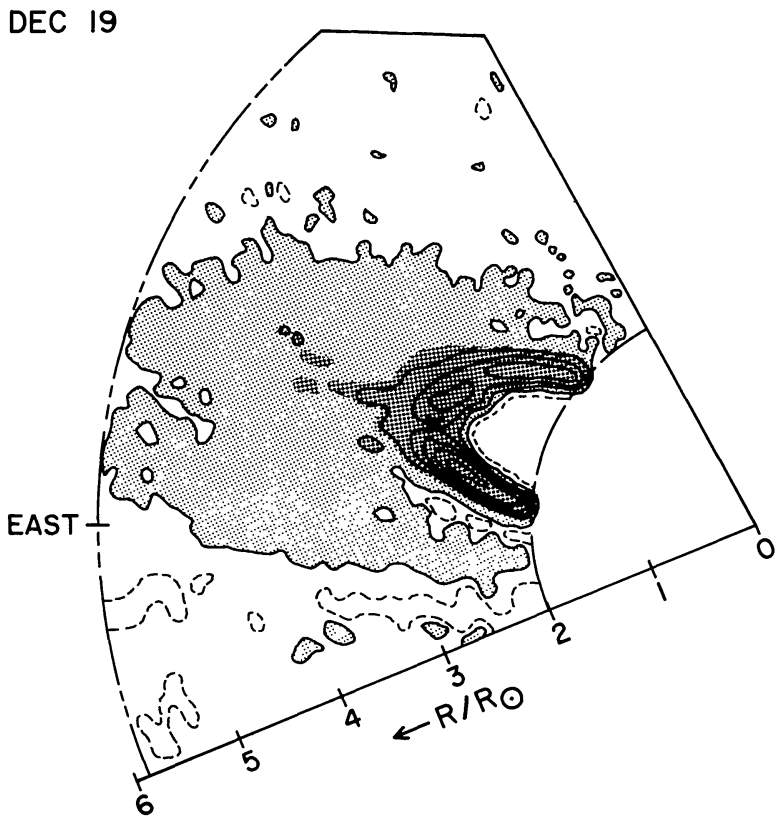

Fig. 2b. An image obtained at 05 : 44 UT has been digitally subtracted from the image of Figure 2a; the resultant image converted to units of excess columnar density is displayed to the same scale and orientation as in Figure 2a. The resolution of the resultant image 2b is degraded to 120 arc s by averaging. Intervals between solid contour lines are 50×10^{-9} g cm^{-2}; the lowest contour level is 6×10^{-9} g cm^{-2}. The dashed contour outlines 'densities' less than -6×10^{-9} g cm^{-2}. In this subtraction, the transient's forerunner (lightly stippled area) extends all the way to the outer edge of the field of view, $2R_\odot$ higher than the transient's leading edge. The X in the darkly stippled area marks the inferred height of maximum excess density at the top of the event.

Figure 2 indicates to us that forerunners probably have configurations similar to their underlying transients.

We have listed in Table I the 21 events recorded by the Skylab coronagraph which have been digitally analyzed and have either good or probable evidence of a forerunner (column 2). A factor of 2 or more change in the radial gradient of excess columnar density at the transient's leading edge is indicated by a 'yes' in column 3. Integration of the excess columnar density between 2 and $6R_\odot$ gives the total excess mass of the event as listed in column 4. The quoted masses are probably lower limits to the total amount of ejected mass because: (1) the coronagraph can not observe below $2R_\odot$ or above $6R_\odot$; (2) it is not known with certainty if or for how long mass continues to flow upward after the outermost material leaves the field of view; and (3) not all the additional material in the corona is in the plane of the sky. Errors in determining the mass difference between any two particular frames, one of which shows a transient, vary from event to event but are generally less than 15% of the event's mass. Previously published masses for some events differ from those given in

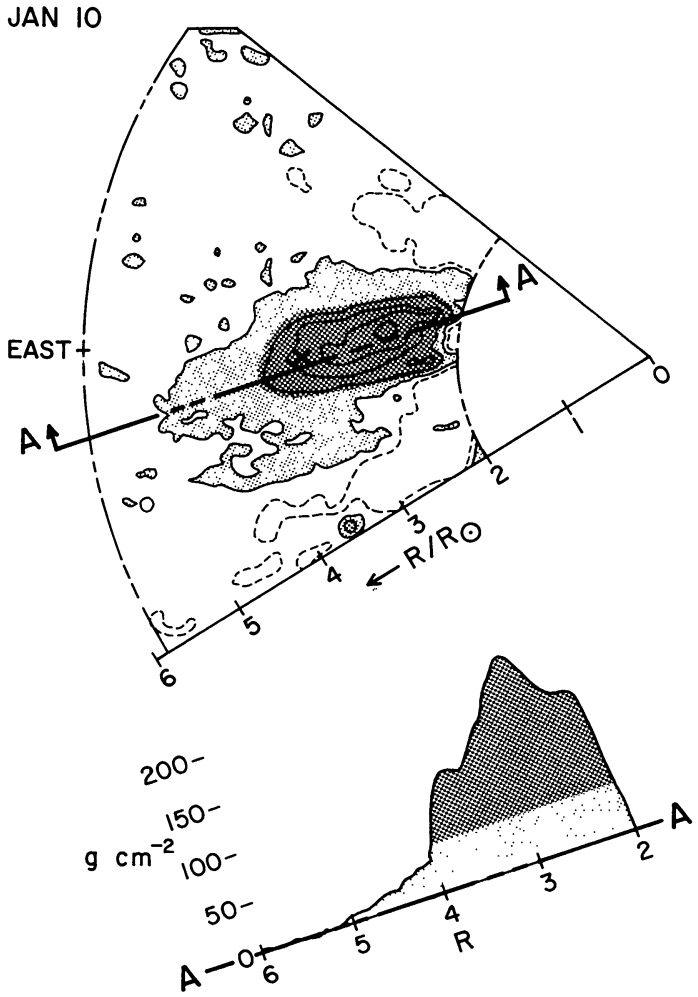

Figure 2c. The event of 10 January 1974 depicted in the same way as Figure 2b with solar north at the top, east to the left. The transient leading edge is at $4R_\odot$ moving outward with a speed of approximately 400 km s^{-1}. The inset at the bottom shows the run of excess columnar density (in units of 10^{-9} g cm^{-2}) along the scan marked A–A.

column 4 for at least two reasons: in the previous work (1) different images were subtracted; and/or (2) the integration of excess columnar densities was carried out over a different area.

To a degree, the measurement of the mass of a transient event is subjective; the beginning of an event, and thus the choice of a pre-transient image to subtract from the event image, and the coronal areas disturbed by the event are occasionally matters of choice. The discovery of forerunners has caused ideas about both the beginning and the size of events to be modified. The differences between the masses presented in this paper and those published earlier indicate the overall accuracy of excess masses independently determined from the same data set. The forerunner mass estimates given in column 5 are determined by integrating the excess columnar density over the area outside the transient (all areas with excess columnar density less than 50×10^{-9} g cm^{-2} including the lightly stippled area in Figures 2b–d but excluding areas beneath the transient). Comparison of the forerunner's to the event's total

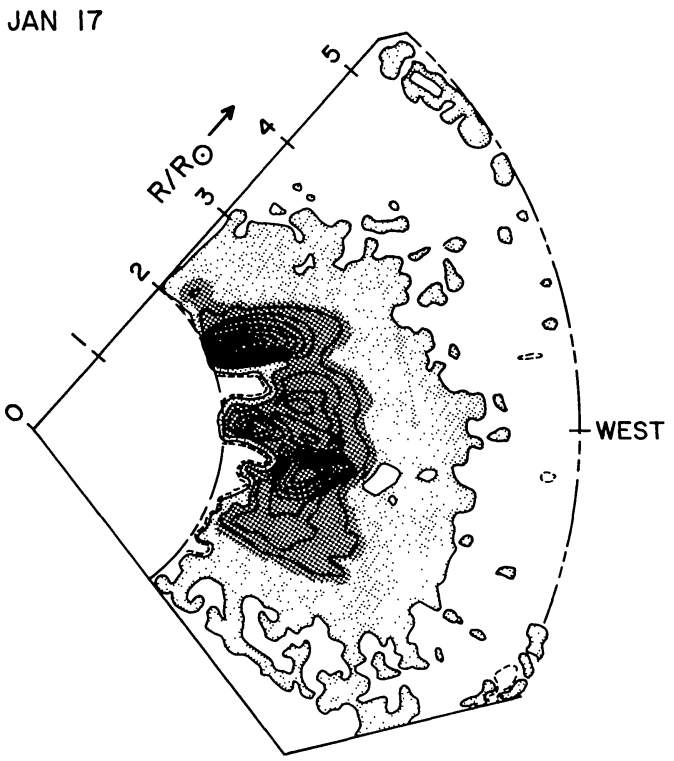

Fig. 2d. The event of 17 January 1974 in the same format as Figure 2b. North is to the top, west to the right. The transient's leading edge is at $3.5R_\odot$ moving outward at approximately 850 km s^{-1}.

excess mass is given by the ratio formed in column 6. For the events that have unquestioned observations of forerunners, this ratio varies from 0.09 to 0.25 with an average of 0.15.

Forerunners are associated with transients of greatly different speeds. Because transient structures sometimes accelerate in the coronagraph's field of view (Gosling *et al.*, 1976), and because the speed of material within a transient may not be the same as the structure speed (for example see Anzer and Poland, 1978), we choose to specify each transient's speed using a well defined location within the transient as follows: a location within a transient that can generally be well determined is the inferred position of maximum excess columnar density at the top of the event. If the transient appears loop-like, this position is within the outermost loop at its top; if blob-like, the center of the blob is chosen. For those few events which have two legs bending toward each other but not closing at the top of the transient, we choose the midpoint between the legs at their tops. This position for each of the three events of Figure 2 is marked by an *X*. An estimate of the apparent upward motion of this point as it passes $3R_\odot$ is listed in column 7 of Table I. Speed estimates are interpolations for most events, and the less accurate measurements are noted in the table.

The table also gives the forerunner offset, defined as the distance between the forerunner's outer edge at the 6×10^{-9} g cm^{-2} excess density contour level. For those events with adequate data, the speeds of the forerunners' outermost edges appear to closely match the speeds of their underlying transients, so that the same offset is

TABLE I

Event	Forerunner observation	Distinct transient/ forerunner boundary	Total excess mass (10^{14} g)	Forerunner excess mass (10^{14} g)	Mass ratio F/T	Transient speed at $3.0R_\odot$ (km s^{-1})	Forerunner offset ($R_\odot$)	Reference
10 Jun	good	yes	38	4	0.11	360	0.7	[1, 2, 3]
24 Jun	good	no	25	3	0.12	60	1.2	[1]
9 Aug[a]	good	no	>10	4?	<0.40?	130[c]	1.0	[1]
10 Aug(A)	good	yes	9	1.5	0.17	50[c]	1.0	
10 Aug(B)	good	yes	42	7	0.17	300	2.0	(1, 3, 4]
13 Aug(A)	good	yes	30	3	0.10	500	1.0	[1]
13 Aug(B)	good	yes	22	2	0.09	175[c]	1.0	[1, 3]
21 Aug	good	yes	50	7	0.15	500	2.0	[1, 3, 5]
26 Aug	probable	no	54[d]	9?	0.17?	150[c]	3.0?	[1, 3, 6]
7 Sept	probable	yes	48	8?	0.17?	200	1.0	[1]
10 Sept	probable	yes	32	4?	0.13?	250	1.0	[1]
15 Sept	good	no	23	5	0.22	600	1.0	[3, 7]
27 Oct	good	no	51	5	0.10	650[c]	1.0	
3 Nov[b]	good	no	>79	13?	0.16?	>1000[c]	1.0	
14 Dec	good	yes	8	2	0.25	500	1.3	[1]
16 Dec	good	yes	32	7	0.22	325	0.7	[1]
19 Dec	good	no	22?	6?	0.27?	90	2.0?	[1, 3, 8]
10 Jan	good	yes	16	2	0.13	400	1.5	[3,9]
12 Jan	good	yes	17	3	0.18	350	1.3	[1, 3]
17 Jan	good	yes	28	5	0.18	600	1.0	[1, 3]
21 Jan		no	36	4	0.11	60	1.5	[1]

[a] This event's quantitative analysis made difficult by instrumental roll.
[b] Portion of event beyond field of view.
[c] Uncertainty in speed of maximum excess density height at $3.0R_\odot > 30\%$.
[d] Reference 6 contains an erroneous mass for this event.

References: [1] Jackson (1979)
[2] Hildner *et al.* (1975a).
[3] Hildner (1977).
[4] Gosling *et al.* (1974).
[5] Poland and Munro (1976).
[6] Hildner *et al.* (1975b).
[7] Dulk *et al.* (1976).
[8] Schmahl and Hildner (1977).
[9] Munro (1978).

approximately maintained within the coronagraph field of view. If anything, the best observations indicate that this forerunner-transient offset decreases somewhat with time. For the 21 events listed, the offsets range from 0.7 to $3.0R_\odot$ and do not seem to be correlated with transient speed or mass.

Do phenomena similar to forerunners occur by themselves without transients? We have digitally analyzed 16 sets of data free of known transients for at least 12 hr before and after the limits of each data set. The cumulative observing time represented by these data sets is approximately 100 hr. In this subset of all coronagraph data, no forerunner-like density enhancements were observed. Compared to the average interval between observed transients of ~47 hr (Munro *et al.*, 1978), this result indicates that 'forerunners' by themselves do not occur frequently – at least not appreciably more often than transients. Indeed, there is no evidence that they ever occur by themselves. Another consequence of this study is that the forerunners discussed in this paper are not frequent, randomly occurring small mass transients only coincidentally associated with the more dense underlying transients.

We have not discovered any case of a transient without a forerunner. Twenty-seven events, more than one-third of the 77 events identified in all the Skylab data by Munro *et al.* (1978), have been analyzed by the digital subtraction technique. The 21 events presented in Table I have data adequate to depict forerunners. The 6 events that were digitally analyzed but not included in the list have data that are inadequate to show whether or not a forerunner existed.

Data adequacy is determined not only by the availability of coronagraph images, but also by our ability to distinguish between K-coronal and other brightness changes present on coronagraph images. A noise background is present in resultant images due to film granularity, the digitization process, and unresolved coronal and stray radiance changes. Non-random noise can be introduced to these data both by the digital reduction process and by variations of the radiance sources which make up the image. Each photograph is scanned with a digital microdensitometer with an aperture of 50 μm diameter (equivalent to 24 arc sec). The measured density is converted to intensity by fitting a density to illumination transfer (D-log E) curve for each coronagraph image. Errors involved in fitting these curves can systematically offset the resultant image values.

Typically, between 4 and $6R_\odot$ the most intense recorded component in the coronagraph images is F-coronal radiance (e.g., Saito *et al.*, 1977). Instrumentally induced stray radiance becomes comparable to other sources of image intensity below $2R_\odot$ (Csoeke-Poeckh *et al.*, 1977). Changes in these two radiance sources on time scales comparable to transient K-coronal events could cause improper determination of the K-corona signal. F-coronal radiance variability over time periods of hours is known to be less than $2 \times 10^{-11}\, B_\odot$ from 4 to $6R_\odot$ (Munro *et al.*, 1975) and is assumed zero here.

Unlike F-coronal radiance, stray radiance can be shown to vary with telescope pointing and occulting disk motions by as much as $2 \times 10^{-9}\, B_\odot$ at $2R_\odot$ (Saito, 1976). It is obvious that the best subtractions are obtained when coronagraph pointing and

occulting disk positions are identical for all images during an event. The most common cause of poor digital subtractions is a roll about the instrument–sun axis between differenced frames, because stray radiance is different at various positions within the coronagraph's field of view and is determined to only ±15% (Csoeke-Poeckh *et al.*, 1977) at any one position. We find that subtraction of images differing in roll by 10 degrees or more does not provide good resultant images. Of course, the effects of improper stray radiance removal are largest near the coronagraph occulting disk where stray radiance is the most intense. Thus, data adequacy is determined by a combination of many factors which add both random and systematic noise to a resultant digital subtraction.

The precision with which coronal brightness changes are determined can be inferred by subtracting coronal photographs separated by time intervals similar to those used in the digital analysis of transients. On the resultant images we determine a 'noise background' in coronal areas free from any known transient effects. If our data were free from random and systematic effects, this noise background would be zero in areas of the images where the *K*-corona was unchanging. The noise background at each point of the resultant image can be expressed as a fraction of the total recorded radiance at that point on the first (subtracted) image. The histogram of Figure 3 shows the noise background for the digitized points of two resultant images. Each point plotted on the histogram represents a 5×5 average of neighboring pixels; thus, the figure is appropriate to resultant images with an angular resolution of 120 by 120 arc sec, the same resolution as the resultant images of Figure 2b–d. The distribution of noise approximates a gaussian distribution centered about zero, and the 2σ level of the noise is at a relative intensity value of ±0.02. The noise

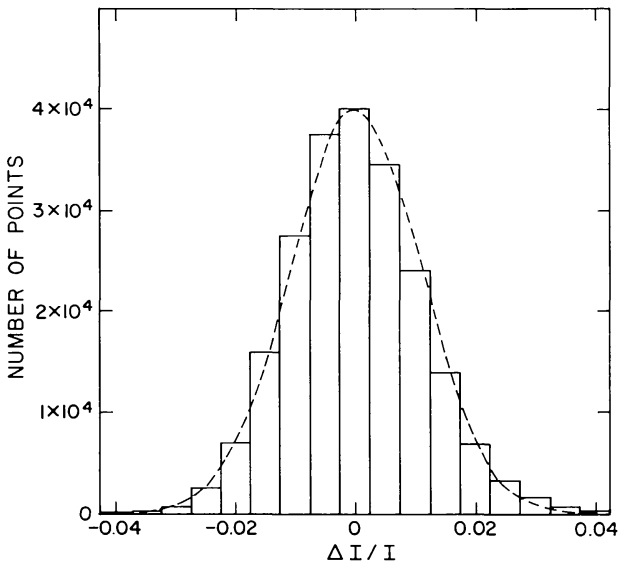

Fig. 3. The number of points versus their relative radiance differences ($\Delta I/I$) for two typical digital subtractions of apparently unchanging coronal images. Each point represents the running average of 25 neighboring pixels (an area 120×120 arc sec^2). The dashed line depicts a zero-centered gaussian fit to the histogram values. $\Delta I/I = 0.02$ corresponds to the 2σ noise level.

distribution is similar for both resultant images and varies only slightly with position within an image.

This $\Delta I/I = 0.02$ Skylab coronagraph noise background, when expressed in units of excess columnar density in the plane of the sky, is almost independent of height for equatorial regions of the corona between 3 and $6R_\odot$ as shown in Figure 4. Latitudinal variations in the 2σ noise level are generally less than ±20%. Thus, an equivalent excess density at 6×10^{-9} g cm^{-2} approximates the 2σ noise background over the major portion of the resultant image formed from the digital subtraction of coronagraph images.

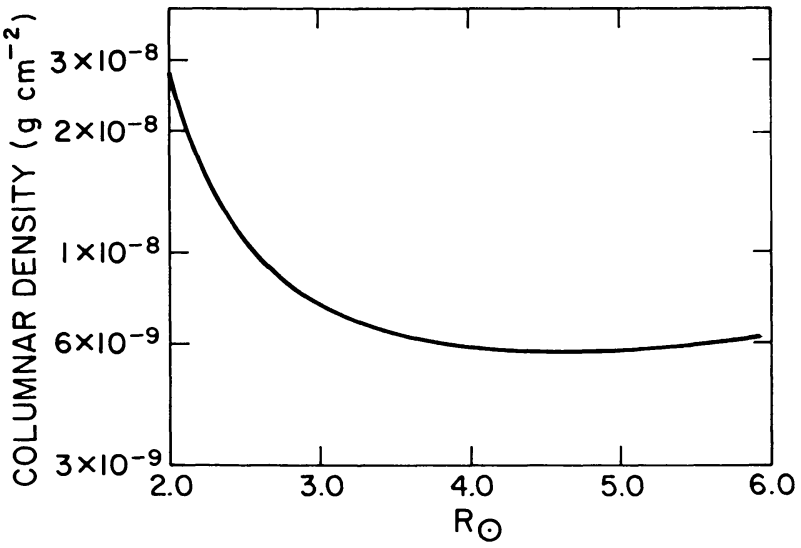

Fig. 4. A depiction of the 2σ noise level ($\Delta I/I = 0.02$) in terms of excess columnar density as a function of radius for Skylab coronagraph images.

Three arguments show that the faint rim of material around each transient is not instrumental in origin.

(1) Several events show evidence of a forerunner long before the brightest portion of the transient comes into the coronagraph field of view. In these events there is no sudden change in the appearance of the forerunner as the transient rises above the occulting disk. Jackson (1979) shows examples of this gradual evolution.

(2) An incorrect film intensity calibration (an error in the D-log E curve at relevant exposure levels) might cause an artificial rim to appear around a transient. However, the 10 January event analyzed with photographs of normal exposure and again with photographs of three times the normal exposure yielded nearly identical results.

(3) Finally, we examined the broad streaks produced on some images by sunlit contaminant particles drifting through the coronagraph's field of view. The streaks chosen are much brighter than normal transients and are only slightly smaller in dimension. Digital subtractions for two of these 'events' show no indication of a halo of light around the contamination streak. Transient to forerunner brightness ratios

are about 10; streak to coronal background brightness ratios are over 100. Thus, any instrumental halo contribution to the forerunner is certainly less than one-tenth of the forerunner brightness.

3. Discussion

We believe that forerunners can not be explained simply as the translation of overlying material, with some mild stretching, from the lower to the upper corona ahead of the transient. In this section we will show why such a mechanism to account for a forerunner is implausible, and briefly mention three other possible scenarios to account for forerunners.

To show that simple translation of material overlying transients to account for forerunners is implausible, from a very simple model of such a translation we calculate the excess densities which would be observed and show that these densities far exceed the densities which are actually observed. The model assumes that a coherent blob of material, initially like its surroundings, is lifted through the coronagraph's field of view, replacing the ambient corona. The material within the blob is constrained to move radially outward from the Sun in such a way that the density within the blob remains uniform. If all the material within the blob moves at the same speed, then the density in the blob varies as $(r/r_0)^2$ where r is the height attained at any one time and r_0 is the blob's starting height. We also investigate a rising blob whose density varies as $(r/r_0)^3$ to mimic the situation where the blob's leading edge is rising faster than its trailing edge.

For the ambient coronal electron density we take

$$N_e(r) = 1.68\times 10^8 r^{-6.13} + 1.36\times 10^6 r^{-2.14}\ (\mathrm{cm}^{-3}),$$
$$2.5 \le r \le 5.5 R_\odot, \tag{1}$$

from the work of Saito *et al.* (1977) and extrapolate down to $r = 1.2R_\odot$. (Such an extrapolation gives results similar to the coronal densities derived earlier by Saito (1970) from a compilation of eclipse observations.) Equation (1) can be considered as a lower limit to the densities actually present in the corona where transients and forerunners occur. Choosing an r_0 and using Equation (1) gives the initial density of the blob, $N_e(r_0)$.

Now the blob is allowed to rise and replace the ambient corona. Along a line of sight passed through the blob when it reaches height $r(R_0)$, the columnar excess density is

$$\rho(r) = Cr\theta[N_e(r_0)f(r) - N_e(r)]\ (\mathrm{g\ cm}^{-2}), \tag{2}$$

where $C = 1.4\times 10^{-13}$ (g cm $R_\odot^{-1}$) is a constant incorporating the effective mass per electron (2×10^{24} g) and the solar radius in centimeters, θ is the angle in radians subtended by the blob at the center of the Sun, and $f(r) = (r/r_0)^n$ describes the internal motion of blob material as described in a preceding paragraph. Although n is a free parameter, $n = 2$ and $n = 3$ seem to be reasonable, and we take $\theta = 30°$.

The excess columnar density predicted for a line of sight passing through the blob has been plotted in Figures 5a (for $n = 2$) and 5b (for $n = 3$), for several initial starting heights r_0. In some events the outer edge of the forerunner appears to arise from below $2.2R_\odot$ with approximately the same speed as the ensuing transient (Jackson, 1979). Figures 5a and b show that coronal material starting at $r_0 \lesssim 2.2R_\odot$ ahead of the transient would be far more dense than the outer edges of the forerunners depicted in Figure 2. For instance, a 30° blob of material expanding as $n = 3$ from below $2.2R_\odot$ has a density of 5×10^{-8} g cm^{-2} at $4.0R_\odot$, ten times more dense than the material at the outer edges of forerunners. Thus, coherent translation of material from the lower ($\lesssim 2.2R_\odot$) corona with only mild stretching ($n = 2$, $n = 3$) above transients does not account for the appearance of forerunners.

Although this result is, admittedly, coronal model dependent, Equation (1) describes a minimum equatorial density model; predicted and observed densities are even more discrepant if we consider coherent upward motion beginning in areas of steeper radial gradients or from within pre-existing dense structures. Coherent, translated blobs which are sufficiently thin in the line-of-sight would match the observations, but coherent outward motion of a thin blob (subtending $\theta < 10°$ at Sun center) of coronal material seems unlikely; there is no observational evidence for extremely thin forerunners, even for the 10 January 1974 transient which is seen edge-on (Figure 2c) and is surrounded by a $\theta \simeq 20°$ to 35° forerunner.

If a forerunner is not merely a coherent translation of material from low to high heights in front of the underlying transient, then local material motions within the forerunner structure are important. At least three possibilities exist. (1) Mouschovias and Poland (1978) suggest that forerunners arise from the compression of ambient coronal magnetic field and its frozen-in material ahead of a rising loop transient. (2) In numerical models of transients, Wu *et al.* (1978) show coronal density enhancements behind the shocks which are driven by the rising transients acting as pistons. Dryer *et al.* (1977) claim that these density enhancements may be identified as forerunners. (3) Another interpretation is that the additional density in a forerunner results from layered material driven upward piecemeal (the outermost part first) with an extreme stretching from the front of a more dense structure. These motions could occur over a relatively long period of time, perhaps hours, and give the appearance of overall, average, organized outward motion of material fairly high in the corona. This third interpretation is suggested by Jackson's (1979) observations that show outward material motion high in the corona long in advance of the surface Hα eruption associated with the event. It should be noted that in the Mouschovias and Poland (1978) and Dryer *et al.* (1977) interpretations, forerunners are not necessarily material ejected during the event, but are comprised of pre-existing corona compressed *in situ*. Coronal material within forerunners may participate in the compression, but then may rise more slowly than and be left behind by forerunner structures; that is, the forerunner pattern speed may be greater than the forerunner material speed. By contrast, in interpretation (3), a forerunner is not merely the consequence of a transient's motion, but is intimately associated with the causes of

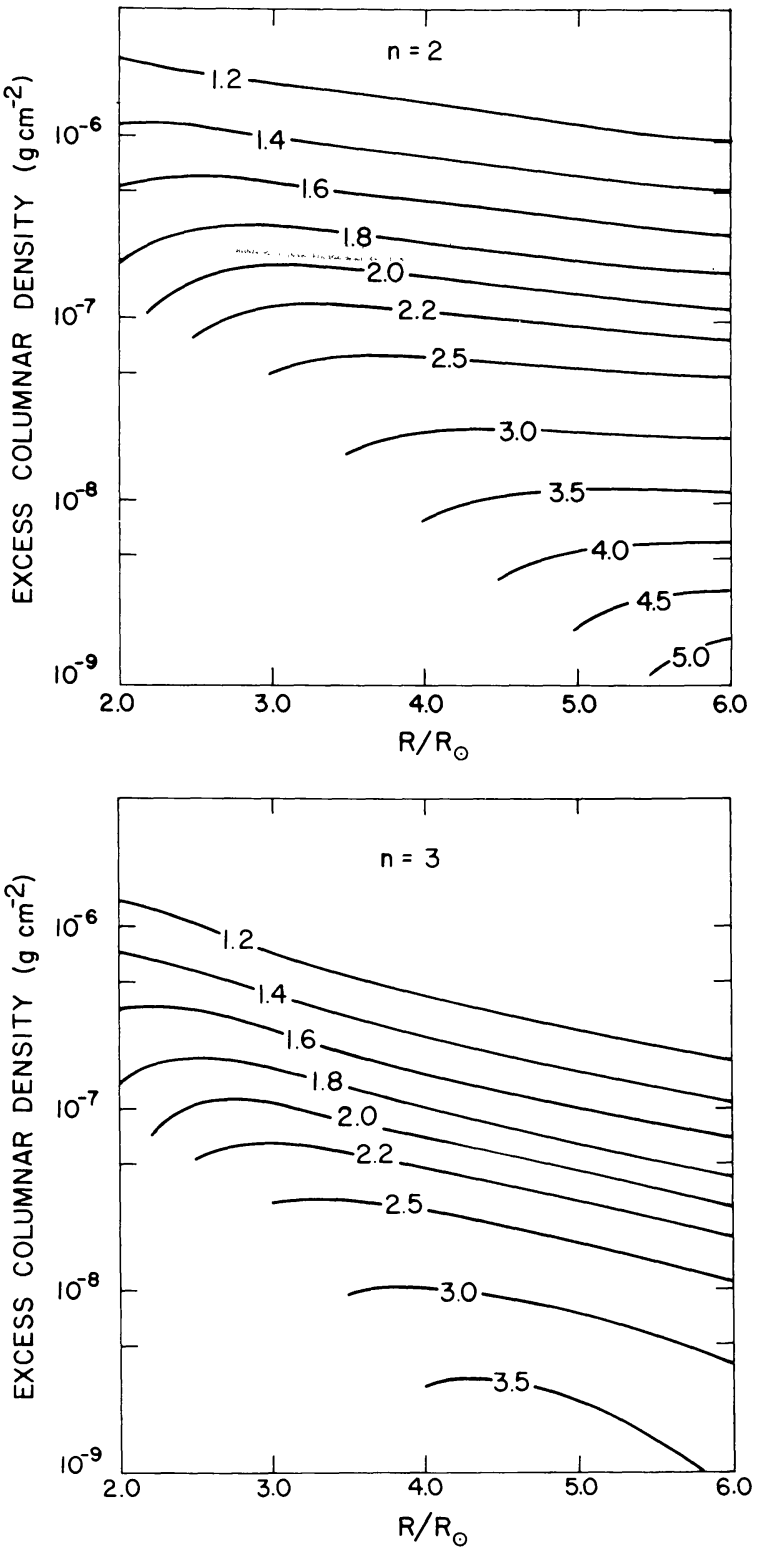

Fig. 5. Excess columnar density which would be observed looking through a blob of material which rises coherently from the lower corona and replaces the ambient plasma as described in the text. For a blob which rises to the height given on the abscissa, each curve shows the predicted excess density which would be observed if the blob started from the height (r_0) indicated on the curve. (a) is plotted for rising material expanding as r^2, and (b) is for rising material expanding as r^3.

the transient and may actually precede the origin of the transient in both space and time.

A definitive modeling study to choose the best interpretation of the observations has not yet been done and is not attempted here. It is obvious that the existence of forerunners must eventually be explained by transient ejection models (see Jackson, 1979 for comments on ejection models published to date). Both better observations, especially of the corona below $2.0R_{\odot}$, and more realistic modeling efforts of the coronal response to transient phenomena are needed to determine which, if any, of the suggested ejection mechanisms is the best one for explaining forerunners.

4. Conclusion

Every analyzed blob or loop-like coronal transient for which adequate data are available appears to be rimmed by a forerunner, a region where the corona is slightly more dense than its pre-transient state. The outer boundaries of these forerunners blend gradually into the background corona 1 to $\geq 2R_{\odot}$ above the leading edge of the denser transient (heretofore considered the entire) portion of the event. Forerunners form rims about the edges of transients that appear less extensive at lower heights down to the minimum heights observable, $\sim 2R_{\odot}$. Forerunners appear to have the same spatial configurations as their underlying transients. Also, a forerunner approximately maintains its lead in front of its transient as they rise through the corona together. Forerunners extend to the positions of the streamers observed to bend in advance of the transient's leading edge in some events and are probably part of the same phenomenon. Speeds of the underlying transients and the forerunners vary from less than 100 to over 800 km s^{-1}. The mass of a forerunner can reach 25% of the total excess mass observed in the corona due to the entire event. As yet we have found no forerunner-like density enhancement occurring by itself without a transient. It is difficult to explain the excess densities observed in forerunners as arising from coherent outward motion of a portion of the lower corona; thus, we suggest that forerunners' excess density arises from either compressed *in situ* corona, or from a piecemeal, layered material ejection. In any case, the presence of forerunners constrains some published explanations of coronal mass ejections and must be reckoned with in any future attempts to explain the physics of these events.

5. Acknowledgements

We appreciate the assistance in data interpretation and analysis provided by Gerry Roach, and the many helpful conversations with R. M. MacQueen, A. I. Poland, R. H. Munro, R. R. Fisher, and T. E. Holzer. Special thanks are given to D. Sime for critically reading this manuscript. In carrying out this research, the authors have benefited considerably from their participation in the Skylab Solar Workshop Series on Solar Flares. The Workshops are sponsored by NASA and NSF and managed by

the High Altitude Observatory. The work of E. Hildner was supported under National Aeronautics and Space Administration Contract NAS5-3950 to the University Corporation for Atmospheric Research.

References

Anzer, U. and Poland, A. I.: 1978, *Astrophys. J.*, in press.
Bartels, J.: 1937, *Terrest. Magn.* **42**, 235.
Chapman, S. and Ferraro, V. C. A.: 1931, *Terrest. Magn.* **36**, 77.
Csoeke-Poeckh, A., MacQueen, R. M., and Poland, A. I.: 1977, *Appl. Opt.* **16**, 931.
Dryer, M., Wu, S. T., and Nakagawa, Y.: 1977, personal communication.
Dulk, G. A., Smerd, S. F., MacQueen, R. M., Gosling, J. T., Magun, A., Stewart, R. T., Sheridan, K. V., Robinson, R. D., and Jacques, S.: 1976, *Solar Phys.* **49**, 369.
Gosling, J. T., Hildner, E., MacQueen, R. M., Munro, R. H., Poland, A. I., and Ross, C. L.: 1974, *J. Geophys. Res.* **79**, 4581.
Gosling, J. T., Hildner, E., MacQueen, R. M., Munro, R. H., Poland, A. I., and Ross, C. L.: 1976, *Solar Phys.* **48**, 389.
Hildner, E.: 1977, in M. A. Shea, D. F. Smart, and S. T. Wu (eds.), *Study of Travelling Interplanatary Phenomena 1977*, D. Reidel Publ. Co., Dordrecht, Holland, p. 3.
Hildner, E., Gosling, J. T., MacQueen, R. M. Munro, R. H., Poland, A. I., and Ross, C. L.: 1975a, *Solar Phys.* **42**, 163.
Hildner, E., Gosling, J. T., Hansen, R. T., and Bohlin, J. D.: 1975b, *Solar Phys.* **45**, 363.
Holzer, T. E.: 1977, in C. F. Kennel, L. J. Lanzerotti, and E. N. Parker (eds.), *Solar System Plasma Physics: A Twentieth Anniversary Overview*, North-Holland Publ. Co., Amsterdam, The Netherlands.
Hundhausen, A. J., Bame, S. J., and Montgomery, M. D.: 1970, *J. Geophys. Res.* **75**, 4631.
Jackson, B. V.: 1979, *Solar Phys.*, in preparation.
Koomen, M., Howard, R., Hansen, R., and Hansen, S.: 1974, *Solar Phys.* **34**, 447.
MacQueen, R. M., Gosling, J. T., Hildner, E., Munro, R. H., Poland, A. I., and Ross, C. L.: 1974, *Soc. Photo-Optical Instr. Eng.* **44**, 207.
Mouschovias, T. Ch. and Poland, A. I.: 1978, *Astrophys. J.* **220**, 675.
Munro, R. H.: 1978, personal communication.
Munro, R. H., Gosling, J. T., Hildner, E., MacQueen, R. M., Poland, A. I., Ross, C. L., and Hopfield, A.: 1975, *Planetary Space Sci.* **23**, 1313.
Munro, R. H., Gosling, J. T., Hildner, E., MacQueen, R. M., Poland, A. I., and Ross, C. L.: 1978, *Solar Phys.*, in press.
Poland, A. I. and Munro, R. H.: 1976, *Astrophys. J.* **209**, 927.
Saito, K.: 1970, *Ann. Tokyo Ast. Obs., Ser. 2* **12**, 53.
Saito, K.: 1976, ATM-WLC Technical Memorandum No. 14, HAO/NCAR, Boulder, Colorado.
Saito, K., Poland, A. I., and Munro, R. H.: 1977, *Solar Phys.* **55**, 121.
Schmahl, E. J. and Hildner, E.: 1977, *Solar Phys.* **55**, 473.
Stewart, R. T., McCabe, M. K., Koomen, M. J., Hansen, R. T., and Dulk, G. A.: 1974, *Solar Phys.* **36**, 203.
Tousey, R.: 1973, *Space Res.* **13**, 713.
Wu, S. T., Dryer, M., Nakagawa, Y., and Han, S. M.: 1978, *Astrophys. J.* **219**, 324.